ACS ES&T Water

pubs.acs.org/estwater

Article

Continuous *In Situ* Nutrient Analyzers Pinpoint the Onset and Rate of Internal P Loading under Anoxia in Lake Erie's Central Basin

Hanna S. Anderson, Thomas H. Johengen, Casey M. Godwin,* Heidi Purcell, Peter J. Alsip, Steve A. Ruberg, and Lacey A. Mason

Cite This: *ACS EST Water* 2021, 1, 774–781

Read Online

ACCESS | Metrics & More | Article Recommendations

ABSTRACT: Lake Erie's central basin experiences seasonal anoxia, contributing to internal sediment phosphorus (P) loading and exacerbating eutrophication. The precise conditions required for internal loading are poorly understood. This study constrains the timing and rates of internal P loading using continuous *in situ* temperature, dissolved oxygen (DO), and soluble reactive P (SRP) observations from two sites. SRP concentrations remained low during normoxia (>2 mg of DO L^{-1}) and hypoxia (0–2 mg of DO L^{-1}) but increased abruptly after anoxia for 12–42 h. SRP flux rate estimations varied, likely due to advection and hypolimnion thickness variation, but could still be reasonably quantified. Flux rates and standard errors during anoxia averaged 25.67 ± 5.5 mg m^{-2} day^{-1} at the shallower site and 11.42 ± 2.6 mg m^{-2} day^{-1} at the deeper site. At the shallow site, the anoxic hypolimnion was displaced with normoxic water, causing cessation of P flux until anoxia returned, and higher flux rates resumed immediately (89.1 ± 8.6 mg m^{-2} day^{-1}), suggesting rapid, redox-controlled P desorption from surface sediments. On the basis of our rate and onset findings, the expected anoxic area and duration in the basin could yield an annual internal SRP load comparable to the annual central basin TP tributary load of 10000–11000 metric tonnes.

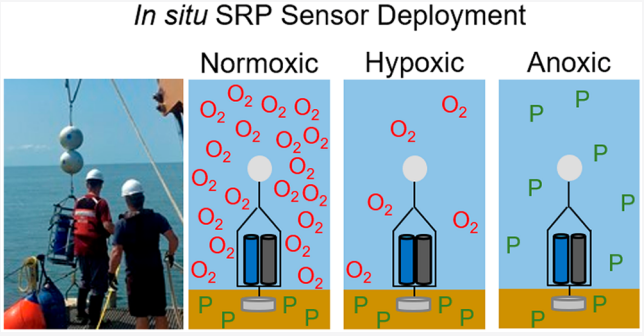

KEYWORDS: *phosphorus, loading, sediment, anoxia, time series, Lake Erie*

INTRODUCTION

Lake Erie is an important and irreplaceable natural resource for its surrounding communities. It provides cities with drinking water, contains vital fisheries for the region, supports the economy, and supplies communities with a source of recreational activities throughout the year. Lake Erie has a history of environmental degradation, and past point source pollutants, including industrial and wastewater discharge, initially led to eutrophication throughout the lake.[1,2] Persistent symptoms of eutrophication include harmful algal blooms (HABs) in the western basin of Lake Erie and seasonal hypoxia in the central basin. Environmental regulations such as the Clean Water Act and the binational Great Lakes Water Quality Agreement (first signed in 1972) forced the management of point source pollution of excess phosphorus (P), and for a time, the ecological consequences of pollution abated or were much diminished.[3,4] However, despite the management of point source nutrient pollution from Lake Erie's watershed, both HABs and hypoxia have re-emerged as problems since the 1990s.[2] More recently, attention has been directed at non-point source pollution, such as P inputs from agriculture and land development. Another source of non-point nutrient loading that is often overlooked is internal phosphorus loading from the lake itself. P associated with settling organic matter accumulates in lake sediment over time.[5] Some of this accumulated P can be released from the sediments to the water during seasonal anoxia, representing an important component of the lake's P budget.[6,7] Internal sediment P loading has been cited as a challenge for achieving long-term removal and P management in lakes,[8,9] including Lake Erie.[10−12] While the literature suggests that internal loading of P due to hypoxia contributes to eutrophication and HABs in Lake Erie,[13,14] the need to understand the biogeochemical conditions that lead to internal P loading remains.

Seasonal hypoxia in Lake Erie's central basin results from a thin hypolimnion (<5 m),[15,16] and consumption of oxygen at the sediment–water interface as organic matter is remineralized.[17−19] The development of seasonal hypoxia impacts redox conditions and leads to P release, magnifying the importance of

Received: September 2, 2020
Revised: January 28, 2021
Accepted: February 1, 2021
Published: February 18, 2021

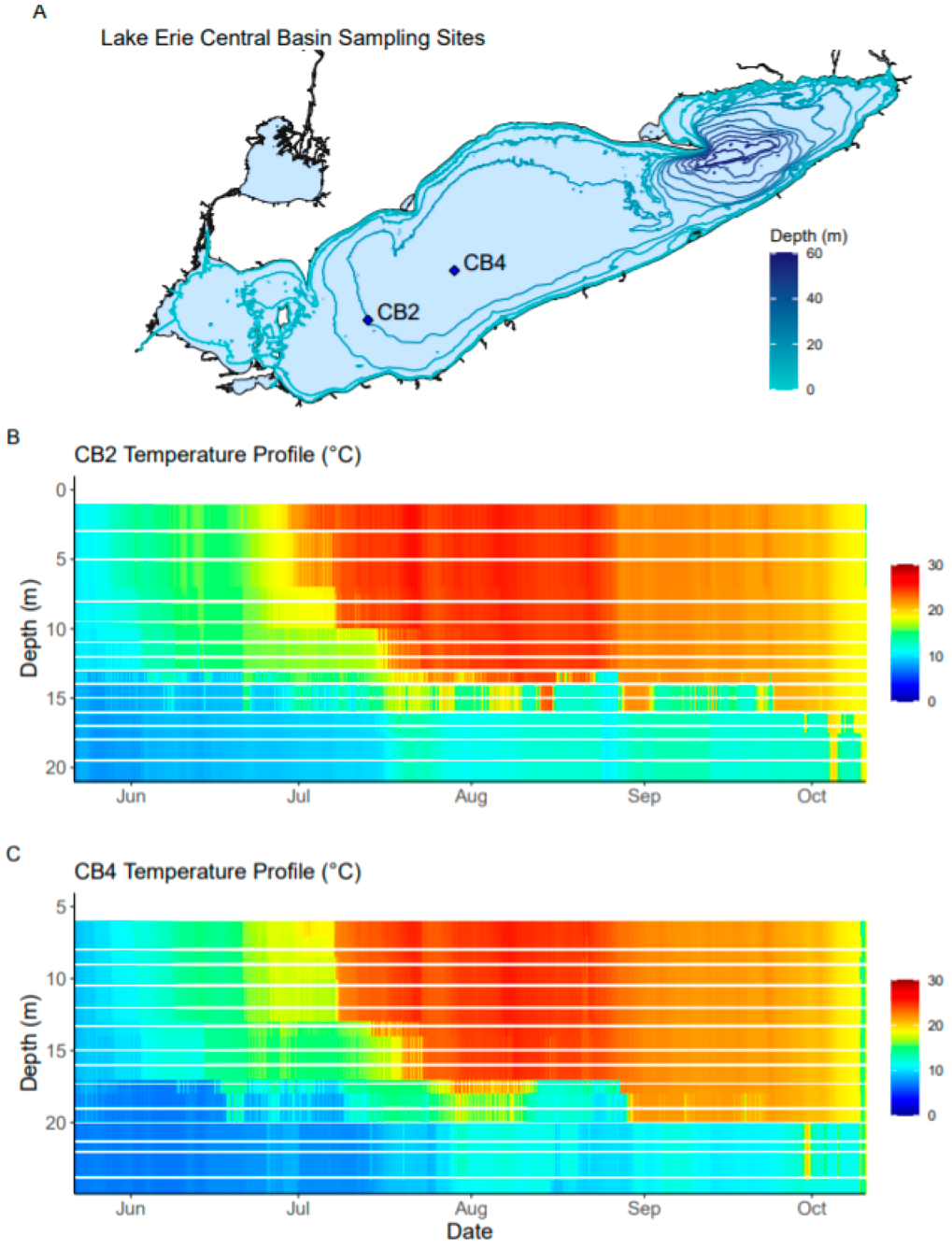

Figure 1. (A) Map of Lake Erie showing mooring stations CB2 and CB4 in Lake Erie's central basin. Heat maps of temperature by depth and date for (B) CB2 and (C) CB4, from May to October 2019, with white horizontal lines indicating sensor placement. Charts were vertically interpolated using depth and temperature data from station moorings.

internal P loading.[20] Under oxic conditions, iron(III) oxyhydroxides are powerful sorbents of inorganic phosphorus,[21] but when dissolved oxygen is depleted, microbes respire these oxides and convert them to a soluble redox state, Fe(II), which no longer sorbs inorganic P.[22,23] This biogeochemical process results in internal P flux, which then comes out of the sediments according to Fickian diffusion principles.[14] P released during internal loading can potentially lead to greater inputs of organic matter production and flux to the sediments, which in turn accelerates oxygen consumption in the hypolimnion. This feedback mechanism, known as "accelerated eutrophication", has been suggested for various water bodies from the Baltic Sea[25] to smaller freshwater−water bodies around the world.[14,24]

Despite the importance of internal P loading to Lake Erie, estimates to quantify this process in the lake are based mostly on laboratory experiments whose ability to represent *in situ* processes is unclear. Previous studies using sediment core incubations under controlled anoxia, pore water concentration profiles, and other methods to estimate P flux reported average flux rates around 6−8 mg m^{-2} day^{-1}.[11,13] Recent sediment core experiments by Anderson computed anoxic flux rates of 5.4−27.6 mg m^{-2} day^{-1}.[26] In addition to constraining the rate of P flux under anoxia, we also need to understand whether P flux begins immediately upon anoxia or exhibits delayed onset.

https://dx.doi.org/10.1021/acsestwater.0c00138
ACS EST Water 2021, 1, 774−781

Several previous lake sediment core studies acknowledge that P flux occurs mainly under anaerobic or anoxic conditions but do not quantify the conditions required for flux onset.[27−29] Anderson showed that P flux from the sediment does not begin until the overlying water becomes completely anoxic and may exhibit a lag of ≤24 h.[26] The observation that P flux begins shortly after the onset of anoxia is critical for estimating the length of time and area of the lake over which internal loading occurs.

The factors affecting internal P loading in Lake Erie are temporally and spatially dynamic, making estimation of site-specific internal P loading challenging. Both modeling forecasts[30] and survey work[31] have shown that the spatial extent and timing of hypoxia and anoxia are highly dynamic in Lake Erie. The result of this dynamic formation of hypoxia and anoxia is that sediments may undergo repeated switching between normoxic and hypoxic conditions and that nearshore areas of the central basin become anoxic before the offshore stations most commonly used to track long-term trends in hypoxia.[32] Previous work has shown that the return of normoxic conditions results in rapid sorption of P back to the sediments, and experiments suggest that positive flux resumes rapidly once anoxia is re-established.[33,26] The hypolimnion of Lake Erie is not static, and hydrodynamic movements can disrupt water column stratification, contributing to the transient nature of anoxia and making it more difficult to quantify internal P loading. Measurements of hypolimnetic soluble reactive P (SRP) from discrete cruises[34,35] confirm that P accumulates within the hypolimnion after anoxia, but the exact onset and flux rate during anoxia are difficult to resolve at a specific location with discrete measurements at intervals of weeks or longer. Lastly, once P diffuses into the water column, it can be assimilated biologically, adsorbed abiotically, and diffused across the thermocline, making it difficult to measure the amount of P that has been released over a given duration at a specific location. These challenges show why net P fluxes are difficult to constrain in large lakes and underscore the need for novel techniques to measure the onset and rate of P flux under *in situ* conditions.

Recent advancements in *in situ* phosphorus analyzers have presented novel sensing techniques and analytical protocols for characterizing P flux at the sediment−water interface.[36] For example, Zorn[37] demonstrated the ability of these analyzers to quantify hypolimnetic P concentration increases between stratification turnover events in Green Bay of Lake Michigan and related these patterns with observed hypolimnetic dissolved oxygen consumption. The study presented here builds upon these previous approaches by using continuous *in situ* monitoring to measure the rates and timing of sediment phosphorus flux at two study sites in Lake Erie's central basin. The application of this novel in situ sensing technology is used here to pinpoint the onset and rate of internal P flux as well as constrain the period of known P flux to anoxic periods. To accomplish these objectives, time series data were collected and analyzed to evaluate SRP flux rates and timing relative to the hypolimnion thickness, DO concentration, and bottom temperature. This study complements and compares results from a parallel study using short-term (5−8 day) sediment core experiment performed at the same sites and time periods.[26]

METHODS

This study involved deploying two WETLab HydroCycle PO4 instruments (SeaBird Scientific, SAS-541861)[38] in Lake Erie's central basin near existing instrumented moorings (stations CB2 and CB4). These instruments are wet chemical sensors engineered for unattended long-term environmental monitoring, while maintaining the required level of sensing frequency and precision for valid, scientifically defensible results. The instrument's stated detection limit is 2.3 μg L^{-1} with a calibrated measurement range of ≤300 μg of SRP L^{-1}. The onboard reagents and NIST traceable calibration standard are stable for 5 months, which adequately covered our intended deployment interval. The central basin is an ideal location for this study as its offshore hypolimnetic waters undergo strong seasonal stratification and are not likely to be affected by tributary sediment inputs, frequent resuspension, or strong mixing, which would affect the accuracy of internal P loading estimates. Water column depths at CB2 and CB4 were 20.5 and 24 m, respectively. The nutrient analyzers were deployed at CB2 on July 24, 2019, and at CB4 on July 25, 2019 (Figure 1), and moored to an anchor weight with the sampling intake 0.5 m above the sediment−water interface. The instruments were programmed to measure SRP concentrations every 6 h until being retrieved October 10, 2019, resulting in >300 measurements at each location over the deployment. Comparison of daily analysis of the built-in NIST traceable standard confirmed stability over the entire deployment.

Temperatures were recorded every 10 min at moorings adjacent to the phosphate analyzer and used to produce water column thermal profiles and estimate the depths of the top and bottom of the metalimnion.[39,40] The hypolimnion thickness was calculated as the difference between the estimated bottom of the metalimnion and the lake bottom. The metalimnion depth was determined by the maximum temperature difference within sequential 1 m depth intervals. The placement of the lowest temperature sensor at both CB2 and CB4 was 0.5 m above the lake bottom. Therefore, the minimum possible hypolimnion thickness that could be resolved was 0.5 m. If the bottom of the metalimnion was not found, the hypolimnion thickness was assumed to be <0.5 m. In these cases, if the difference between the surface and bottom temperatures was <0.5 °C, the water column was considered fully mixed and the hypolimnion thickness was reported to be 0 m.

In this paper, hypoxia is defined by the common definition of <2 mg of DO L^{-1} and anoxia refers to 0 mg of DO L^{-1} conditions. The oxygen sensors (PME miniDOTLoggers) did not register zero when dissolved oxygen was completely absent. Therefore, a non-zero sensor concentration representing zero dissolved oxygen was determined on the basis of (1) the reading of the sensors in a zero-oxygen bath prepared with potassium metabisulfite and confirmed by Winkler titration and (2) flat-line (unchanging at the hundredths place) DO *in situ* readings after the onset of anoxia. The sensor readings used to denote anoxia were 0.03 and 0.13 mg L^{-1} for the sensors at CB2 and CB4, respectively.

The HydroCycle measures SRP using a modified version of the ascorbic acid molybdenum blue reaction, detailed in ref 37. Prior to deployment, the response accuracy and linearity of the HydroCycles were analyzed in the lab via submersion in approximately 180 L of deionized water. The instruments were purged of bubbles and programmed to sample every 20 min. The instruments were run for several hours to equilibrate, and

https://dx.doi.org/10.1021/acsestwater.0c00138
ACS EST Water 2021, 1, 774−781

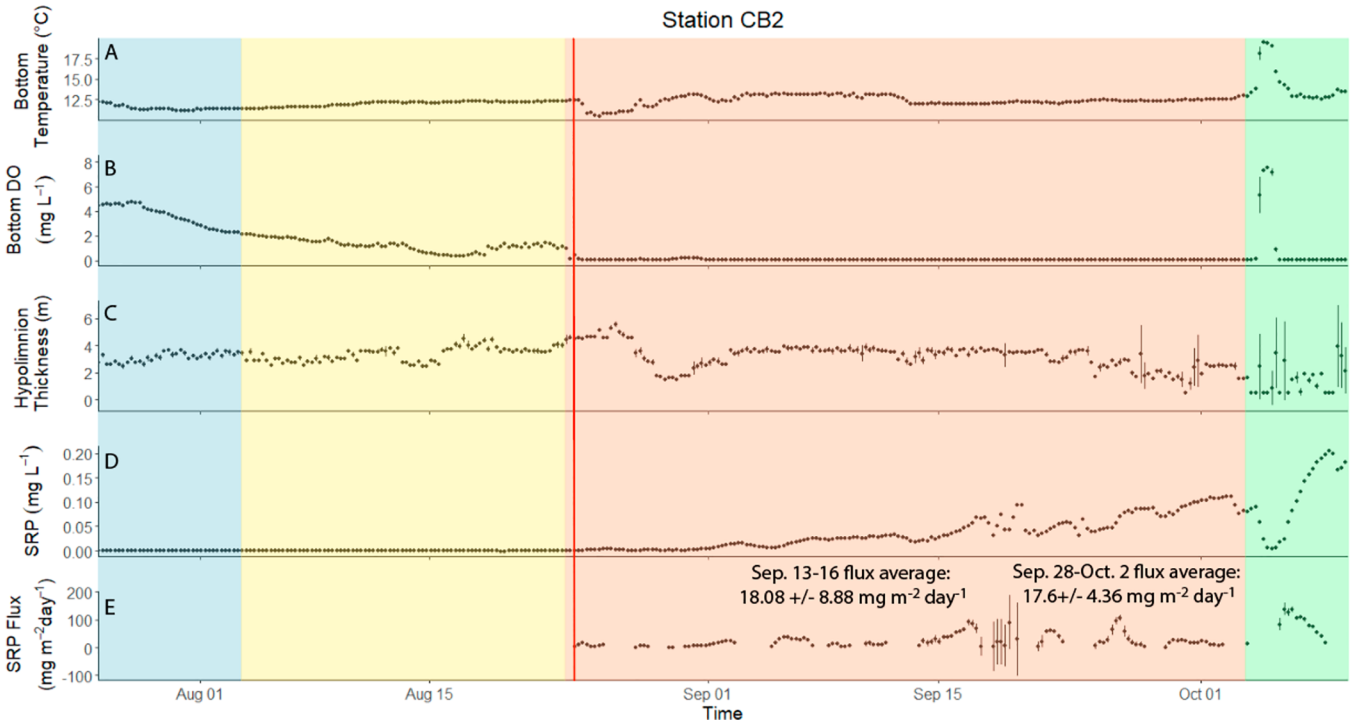

Figure 2. Station CB2 readings of (A) bottom temperature, (B) bottom dissolved oxygen, (C) hypolimnion thickness, (D) SRP concentration, and (E) estimated phosphorus flux for the duration of the HydroCycle monitoring period. Colored phases are explained in the text. Representative average flux estimates are shown in panel E. Error bars refer to the standard deviation of five sequential measurements.

then the concentration of PO_4 in the drum was increased sequentially to 0, 5, 10, 20, and 40 $\mu g\ L^{-1}$ by additions of the NIST-traceable phosphate standard (Hach Co., Loveland, CO). At each concentration, the instruments sampled three times. The corresponding reference samples were analyzed with a Seal AA3 XY-2 autoanalyzer (Seal AA3 AutoAnalyzer Manual) using method G-297-03 revision 5 (Multitest MT 19) against standards generated from the NIST-traceable phosphate standard. The linear regressions of HydroCycle concentration versus reference concentration for each instrument showed underprediction by the HydroCycle. The equations for the lines of best fit were $y = 0.64x + 0.66$ and $y = 0.68x + 0.66$, and the R^2 values were 0.996 and 0.999 for the HydroCycle units for CB2 and CB4, respectively. There was no significant difference in the slopes between the two HydroCycle instruments ($p < 0.05$).

This calibration check was performed to confirm the operational functionality of the instruments and ensure they would respond in a linear relationship to increasing SRP concentrations over the measured range. Reported *in situ* SRP concentrations in this paper were not corrected to the predeployment calibration; rather, they were reported from the HydroCycle factory-set absorbance ratios. Data were not corrected for this difference due to unknown matrix effects of lake water on the reaction relative to deionized type 1 water. To this latter point, it is assumed that any negative concentrations reported by the instrument during the initial period of deployment reflect this difference in calibration and not a systematic error. It was assumed that the HydroCycle measured representative, equilibrated hypolimnion SRP concentrations that could be used to reliably estimate the flux rate.

Phosphorus flux rates were calculated using time series of SRP concentrations and estimated hypolimnion thickness. The "lm" function in R (https://CRAN.R-project.org) was used to create a linear model of SRP with respect to time and was applied over a moving time window of 24 h. Flux estimates and standard errors were derived from five sequential SRP measurements, multiplied by the mean hypolimnion thickness over that interval, and normalized per square meter to generate rates in milligrams per square meter per day. The results were reported at the middle time point of each sequential window. The high frequency of sampling for both SRP and temperature was necessary to ensure the accuracy of rate measurements considering the long-term variability of hypolimnetic conditions. When the estimated SRP concentration change was negative or the confidence interval included zero, no flux rate was reported. On the basis of observations of hypolimnion thickness and temperature change, these intervals most likely represented either normoxic periods, when no detectable flux occurred, or rapid displacement or mixing of local hypolimnetic water rather than an actual reversal in the direction of the sediment P fluxes. For one measurement interval at CB2, a P flux rate of >200 mg m^{-2} day^{-1} was calculated but was not taken to accurately represent a P flux rate. This extreme rate estimate coincided with compression and expansion of the hypolimnion caused by vertical mixing within the water column, which led to exaggerated accumulated mass computations during this time increment.

The lag time in the onset of SRP flux was defined as the time interval between the onset of anoxia and the first cumulative SRP reading that exceeded three standard deviations from the mean of the preceding cumulative measurements.

RESULTS AND DISCUSSION

Continuous temperature data from May to October 2019 reveal the development and progression of thermal stratification at stations CB2 and CB4 (Figure 1). The hypolimnion

https://dx.doi.org/10.1021/acsestwater.0c00138
ACS EST Water 2021, 1, 774−781

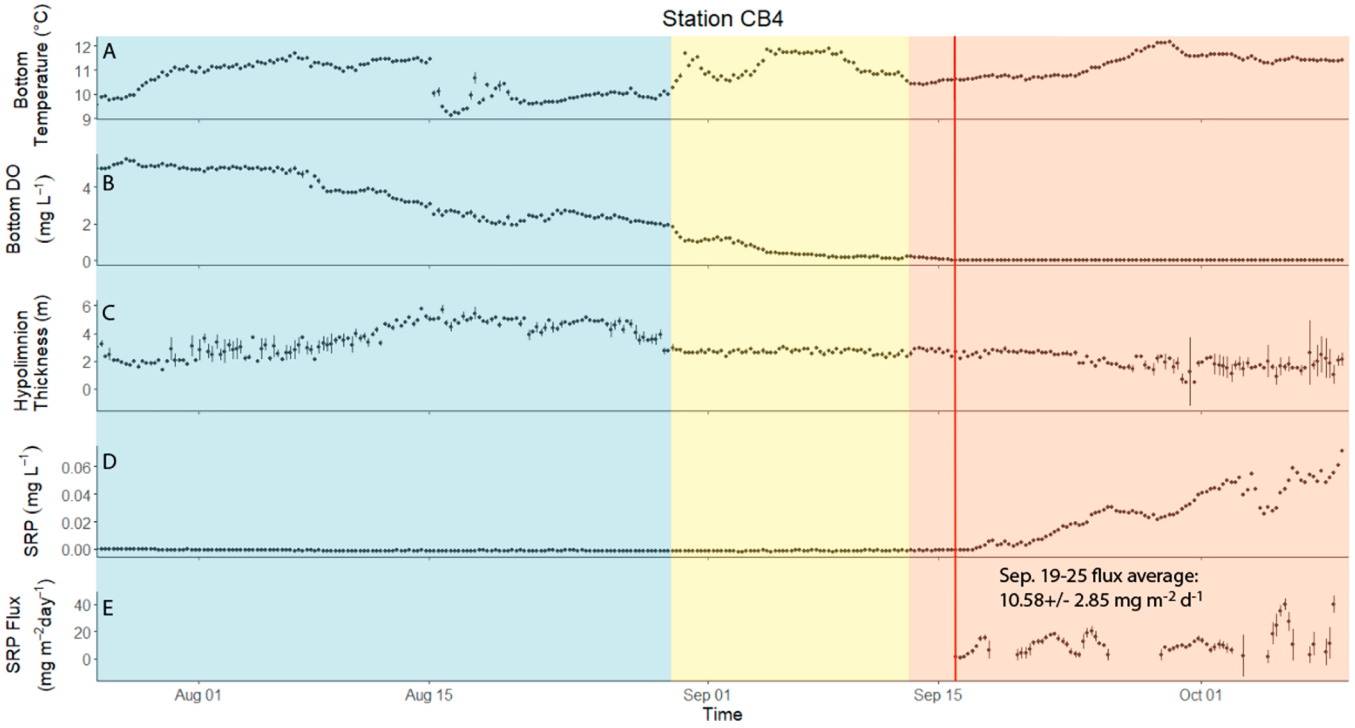

Figure 3. Station CB4 readings of (A) bottom temperature, (B) bottom dissolved oxygen, (C) hypolimnion thickness, (D) SRP concentration, and (E) estimated phosphorus flux for the duration of the HydroCycle monitoring period. Colored phases are explained in the text. Representative average flux estimates are shown in panel E. Error bars refer to the standard deviation of five sequential measurements.

began forming in late June, and by August, a hypolimnion of approximately 3 m was established (Figures 2 and 3). The progression of the deepening thermocline was delayed by several weeks at the deeper, more offshore station, CB4. After thermal stratification occurred, the water columns remained stratified throughout the deployment, with the exception of a mixing event at CB2 beginning on October 3 and lasting approximately 100 h. During this interval, the colder anoxic hypolimnion was displaced by warmer oxygenated water, shown in Figure 1 where 15 °C water reaches the lake bottom. The beginning of another mixing event indicating a full overturn can be seen just before monitoring ends on October 10. This event was not fully characterized by the monitoring period but likely indicated the end of the seasonal stratification.

Time series data of bottom layer temperature, DO, hypolimnion thickness, SRP concentration, and P flux data for stations CB2 and CB4 are given in Figures 2 and 3, respectively. Hypolimnetic conditions during the deployment period can be characterized into phases on the basis of dissolved oxygen and temperature data. The first phase (blue) represents stable lake stratification with a normoxic hypolimnion that lasted between July 24 and August 4 at CB2 and between July 25 and August 28 at CB4. The second phase (yellow) denotes the period of hypoxia with DO concentrations between 0 and 2 mg L^{-1}, which extended until August 23 at CB2 and until September 15 at CB4. During this second phase, SRP concentrations remained low and sediment P flux was not detectable. The third and longest phase (red) represents the period of anoxia with DO concentrations at zero, which lasted until October 3 at CB2 and until October 10 at CB4. SRP concentrations started to increase, and positive P fluxes were observed within 0.5 day of the hypolimnion reaching anoxia at CB2 and within 1.75 days of anoxia at CB4. This flux onset is represented in the figures by the vertical red line within the third phase.

A fourth phase (green) characterizing intermittent disruption of the hypolimnion occurred at only CB2 (Figure 2). This phase was defined by a strong water column mixing event beginning on October 3 when anoxic hypolimnion water was replaced with normoxic water. The mixing event caused both bottom temperature and DO levels (panels A and B, respectively) to increase rapidly indicating a strong downwelling event that produced a completely mixed water column. Once normoxic conditions were established, there was a rapid decline in SRP concentrations to levels measured prior to anoxia, followed by a rapid buildup under SRP conditions once anoxia was re-established after approximately 3 days.

The development of anoxia at station CB4 was slower and occurred ~24 days later than at CB2, reflecting a thicker hypolimnion at the deeper CB4 and a corresponding greater volume to surface area relationship that greatly affects oxygen consumption rates. Specifically, the onset of anoxia occurred on August 23 at 14:05 at CB2 and on September 15 at 20:05 at CB4. Despite the four-week difference in the timing of anoxia onset, the lag time from the onset of anoxia to the onset of SRP flux was similar between stations. The SRP flux lag time was 12 h at CB2 and 42 h at CB4. The high sampling frequency by the HydroCycles (±6 h for the sampling interval) provided relatively fine temporal resolution for these lag time estimates and further corroborated the complementary laboratory core incubation experiments indicating that flux does not begin until after anoxia is fully established.[26] In that study, the anoxic lag time for P flux ranged from 0 to 28.6 h at CB2 and from 1.1 to 10.7 h at CB4. The longer lag time observed at CB4 in comparison to that of the sediment core experiments could be due to the higher *in situ* water volume to

https://dx.doi.org/10.1021/acsestwater.0c00138
ACS EST Water 2021, 1, 774−781

sediment area ratio that causes concentrations to increase more slowly.

Panels E in Figures 2 and 3 show the average P flux rates during the total period of anoxia were 25.7 ± 5.5 mg m^{-2} day^{-1} (range of 1.33−106 mg m^{-2} day^{-1}) at CB2 and 11.4 ± 2.55 mg m^{-2} day^{-1} (range of 0.79−40.1 mg m^{-2} day^{-1}) at CB4. Due to the variability in the hypolimnion volume, average anoxic flux rates were computed for shorter representative date ranges when the hypolimnion thickness was relatively stable and less likely to influence rate estimates. At station CB2, the flux rate average was 18.1 ± 8.9 mg m^{-2} day^{-1} from September 13 to 16 and 17.6 ± 4.4 mg m^{-2} day^{-1} from September 28 to October 2. At station CB4, the flux rate average was 10.6 ± 2.9 mg m^{-2} day^{-1} from September 19 to 25. These estimates are lower than the overall average anoxic flux rates at the respective sites due to the removal of exaggerated flux rates that occurred during hypolimnetic volume fluctuations.

The parallel laboratory sediment core incubation study computed average anoxic P flux rates of 14 mg m^{-2} day^{-1} with a range of 5.4−27.6 mg m^{-2} day^{-1}.[26] This corroborates average *in situ* flux rate measurements from both stations; however, the mean *in situ* flux rate at CB2 is at the high end of the range from the lab experiments. Previous studies reported anoxic P flux rates of 7.6−8 mg m^{-2} day^{-1} from central basin sediment and *in situ* hypolimnion measurements[13] and 6.56 ± 6.05 mg m^{-2} day^{-1} from western basin sediment cores.[11] Gibbons and Bridgeman reported a range of 0.52−5.96 mg m^{-2} day^{-1} for western basin sediment cores incubated at 10 °C.[12] The study of *in situ* flux rates presented here generally corroborates these previous estimates; however, they incorporate a wider range of rates due to the unique monitoring approach of observing flux over the entirety of the season as the water column undergoes changes in DO conditions and hypolimnion thickness.

Outside of these stable periods, flux rates changed rapidly in response to DO concentration during the fourth phase at CB2 (Figure 2) when a mixing event replaced the hypolimnion with normoxic water. The SRP concentration and P flux rates (panels D and E, respectively) initially dropped rapidly until DO levels in the replacement water were depleted to anoxia approximately 100 h after the initial disruption. Within hours of anoxia being re-established, SRP concentrations increased with flux rates ≤3 times faster than previously observed at this site, peaking around October 6 and averaging 89.1 ± 8.6 mg m^{-2} day^{-1} (range of 18.4−137.8 mg m^{-2} day^{-1}), which was 3 and 7 times greater than the average anoxic flux rates at CB2 and CB4, respectively.

While the flux rates observed immediately after the return of anoxia were high, it can be argued that they are feasible and can be explained by a simple mechanism. Specifically, if oxygenated water caused the surface sediments to trap SRP originating from diagenesis and diffusion occurring in lower layers, the return of a low redox potential should have resulted in rapid desorption of P from iron oxides and a high apparent flux rate. To explore whether this mechanism is feasible, we calculated the mass of SRP that would have been released from sediments if they had remained anoxic during the 5 day normoxic mixing event and 2.75 days following the event. If this calculated mass of SRP (205 mg m^{-2}) were released during the 2.75 days following the event, it would produce an expected flux rate of 75 mg m^{-2} day^{-1}, which compares favorably with the observed average flux rate during that interval (89.1 ± 8.6 mg m^{-2} day^{-1}). Additionally, high velocity bottom currents have the potential to cause surface erosion or pore water pumping, increasing SRP release rates under renewed anoxia by exposing subsurface P and encouraging flux. While the hypolimnion was not completely disrupted at CB4 during this mixing event, there was still a noticeable perturbation that interrupted the linear buildup of SRP and produced considerable variation in the flux measurements due to mixing across the thermocline or within the thin hypolimnion.

Laboratory experiments showed a similar phenomenon during reaeration of anoxic cores,[26] suggesting that release of SRP ends abruptly when overlying water is oxygenated.

CONCLUSION

This study's high-frequency sampling showed that positive P flux requires anoxia and begins after a lag time of 12−42 h, meaning there is a portion of time where flux does not occur when it was previously assumed (e.g., during hypoxia). We estimated the magnitude of seasonal basin-wide internal P loading using published estimates for the area of the basin that contributes to internal loading (6435−9000 km^2)[30,32,41] and anoxic hypolimnion exposure timing observed at these two moorings (30 and 50 days). While any such calculation of internal loading is dependent on knowing the area and duration, both of which are poorly constrained by direct observations *in situ*, we present this to illustrate the potential magnitude based on our findings. Using the mean anoxic flux rates from both stations (11.42 and 25.67 mg m^{-2} day^{-1}) and observed anoxic duration, low and high annual internal central basin P loading estimates are 2056−11551 metric tonnes (t) as SRP. The high end of this range equals the approximate external TP loading input from rivers and tributaries, approximately 10000−11000 t annually.[10] Moreover, SRP from internal loading is immediately bioavailable, which would make this contribution much more impactful in terms of exacerbating eutrophication. Environmental managers tasked with tributary load reduction must take internal loading estimates into account when determining how to balance the total P load. Historical and persistent sediment P loading represents a delayed lake response to eutrophication and prevents the successful management of a system when only external P loading is considered.[8] Under the GLWQA, the tributary loading reductions recommended for Lake Erie were developed to meet multiple water quality objectives that include minimizing hypoxia in the central basin. It is difficult to predict how quickly the extent of anoxia in the central basin, and thus internal loading, will respond to decreases in tributary loading. However, due to the potential for internal loading to cause positive feedback impacts on primary production and hypoxia,[4] it will be important to document changes in internal loading that occur as tributary loads are decreased. This could be achieved by the increased frequency of shipboard collection of samples before, during, and after seasonal stratification, but this study shows the potential for describing this progress at greater temporal resolution using autonomous, continuous monitoring instrumentation.

Continued monitoring will be particularly important as climate change lengthens the duration of stratification,[42] leading to increasingly longer periods of hypolimnion anoxia and higher average P flux rates.[12] Future modeling work supported by additional monitoring of hypoxia could use these findings to track interannual loading variability and better constrain the importance of internal loading to this regionally important freshwater resource.

https://dx.doi.org/10.1021/acsestwater.0c00138
ACS EST Water 2021, 1, 774−781

AUTHOR INFORMATION

Corresponding Author

Casey M. Godwin − *Cooperative Institute for Great Lakes Research (CIGLR), School for Environment and Sustainability, University of Michigan, Ann Arbor, Michigan 48109-1041, United States;* orcid.org/0000-0002-4454-7521; Email: cgodwin@umich.edu

Authors

Hanna S. Anderson − *Cooperative Institute for Great Lakes Research (CIGLR), School for Environment and Sustainability, University of Michigan, Ann Arbor, Michigan 48109-1041, United States*

Thomas H. Johengen − *Cooperative Institute for Great Lakes Research (CIGLR), School for Environment and Sustainability, University of Michigan, Ann Arbor, Michigan 48109-1041, United States;* orcid.org/0000-0002-3596-5457

Heidi Purcell − *Cooperative Institute for Great Lakes Research (CIGLR), School for Environment and Sustainability, University of Michigan, Ann Arbor, Michigan 48109-1041, United States*

Peter J. Alsip − *Cooperative Institute for Great Lakes Research (CIGLR), School for Environment and Sustainability, University of Michigan, Ann Arbor, Michigan 48109-1041, United States*

Steve A. Ruberg − *Great Lakes Environmental Research Laboratory, National Oceanic and Atmospheric Administration, Ann Arbor, Michigan 48108, United States*

Lacey A. Mason − *Great Lakes Environmental Research Laboratory, National Oceanic and Atmospheric Administration, Ann Arbor, Michigan 48108, United States*

Complete contact information is available at: https://pubs.acs.org/10.1021/acsestwater.0c00138

Notes

The authors declare no competing financial interest.

ACKNOWLEDGMENTS

This is CHRP contribution 254 and NOAA-GLERL contribution 1972. Funding was awarded to the Cooperative Institute for Great Lakes Research (CIGLR) through the NOAA Cooperative Agreement with the University of Michigan (NA17OAR4320152). This is CIGLR contribution 1173. This work was supported by the National Oceanic and Atmospheric Administration's National Centers for Coastal Ocean Science Competitive Research Program under Grant NA16NOS4780209 to the University of Michigan and through the NOAA Cooperative Agreement with the Cooperative Institute for Great Lakes Research (CIGLR) at the University of Michigan (NA17OAR4320152). The authors thank two anonymous reviewers for comments that improved the manuscript.

REFERENCES

(1) DePinto, J.; Young, T.; Martin, S. Algal-Available Phosphorus in Suspended Sediments from Lower Great Lakes Tributaries. *J. Great Lakes Res.* **1981**, *7* (3), 311−325.

(2) Scavia, D.; David Allan, J.; Arend, K. K.; Bartell, S.; Beletsky, D.; Bosch, N. S.; Brandt, S. B.; Briland, R.; Daloğlu, I.; DePinto, J.; Dolan, D.; Evans, M. A.; Farmer, T.; Goto, D.; Han, H.; Höök, T.; Knight, R.; Ludsin, S.; Mason, D.; Michalak, A.; Richards, P.; Roberts, J.; Rucinski, D.; Rutherford, E.; Schwab, D.; Sesterhenn, T.; Zhang, H.; Zhou, Y. Assessing and addressing the re-eutrophication of Lake Erie: Central basin hypoxia. *J. Great Lakes Res.* **2014**, *40* (2), 226−246.

(3) Federal Water Pollution Control Act (Clean Water Act, CWA). 1972. U.S. Government. https://www.gpo.gov/fdsys/pkg/USCODE-2017-title33/html/USCODE-2017-title33-chap26.htm (accessed 2020-04-12).

(4) Great Lakes Water Quality Agreement (GLWQA). Protocol amending the agreement between the United States of America and Canada on Great Lakes water quality. 2012. https://www.epa.gov/glwqa.

(5) Gerling, A.; Munger, Z.; Doubek, J.; Hamre, K.; Gantzer, P.; Little, J.; Carey, C. Whole-Catchment Manipulations of Internal and External Loading Reveal the Sensitivity of a Century-Old Reservoir to Hypoxia. *Ecosystems* **2016**, *19*, 555−571.

(6) Nürnberg, G. The prediction of internal phosphorus load in lakes with anoxic hypolimnia. *Limnol. Oceanogr.* **1984**, *29* (1), 111−124.

(7) Nürnberg, G. Phosphorus from internal sources in the Laurentian Great Lakes, and the concept of threshold external load. *J. Great Lakes Res.* **1991**, *17* (1), 132−140.

(8) Giles, C.; Isles, P.; Manley, T.; Xu, Y.; Druschel, G.; Schroth, A. The mobility of phosphorus, iron, and manganese through the sediment-water continuum of a shallow eutrophic freshwater lake under stratified and mixed water-column conditions. *Biogeochemistry* **2016**, *127*, 15−34.

(9) Mohamed, M. N.; Wellen, C.; Parsons, C. T.; Taylor, W. D.; Arhonditsis, G.; Chomicki, K. M.; Boyd, D.; Weidman, P.; Mundle, S. O. C.; Van Cappellen, P.; Sharpley, A. N.; Haffner, D. G. Understanding and managing the re-eutrophication of Lake Erie: Knowledge gaps and research priorities. *Freshwater Science* **2019**, *38*, 675.

(10) Paytan, A.; Roberts, K.; Watson, S.; Peek, S.; Chuang, P.-C.; Defforey, D.; Kendall, C. Internal loading of phosphate in Lake Erie Central Basin. *Sci. Total Environ.* **2017**, *579*, 1356−1365.

(11) Matisoff, G.; Kaltenberg, E.; Steely, R.; Hummel, S.; Seo, J.; Gibbons, K.; Bridgeman, T.; Seo, Y.; Behbahani, M.; James, W.; Johnson, L.; Doan, P.; Dittrich, M.; Evans, M. A.; Chaffin, J. Internal loading of phosphorus in western Lake Erie. *J. Great Lakes Res.* **2016**, *42*, 775−788.

(12) Gibbons, K. J.; Bridgeman, T. B. Effect of temperature on phosphorus flux from anoxic western Lake Erie sediments. *Water Res.* **2020**, *182*, 116022.

(13) Nürnberg, G.; Howell, T.; Palmer, M. Long-term impact of Central Basin hypoxia and internal phosphorus loading on north shore water quality in Lake Erie. *Inland Waters* **2019**, *9*, 362.

(14) Steinman, A.; Spears, B. Chapter 1: What Is Internal Phosphorus and Why Does It Occur?; Chapter 19: Internal Loading of Phosphorus to Lake Erie: Significance, Measurement Methods, and Available Data. *Internal Phosphorus Loading in Lakes: Causes, Case Studies, and Management*; J. Ross Publishing, 2020.

(15) Beletsky, D.; Hawley, N.; Rao, Y. R.; Vanderploeg, H. A.; Beletsky, R.; Schwab, D. J.; Ruberg, S. A. Summer thermal structure and anticyclonic circulation of Lake Erie. *Geophys. Res. Lett.* **2012**, *39* (6), n/a.

(16) Burns, N. Oxygen Depletion in the Central and Eastern Basins of Lake Erie, 1970. *J. Fish. Res. Board Can.* **1976**, *33* (3), 512−519.

(17) Smith, D. A.; Matisoff, G. Sediment oxygen demand in the central basin of Lake Erie. *J. Great Lakes Res.* **2008**, *34*, 731−744.

(18) Snodgrass, W. Analysis of models and measurements for sediment oxygen demand in Lake Erie. *J. Great Lakes Res.* **1987**, *13*, 738−756.

(19) Snodgrass, W.; Fay, L. Values of Sediment Oxygen Demand Measured in the Central Basin of Lake Erie, 1979. *J. Great Lakes Res.* **1987**, *13* (4), 724−730.

(20) Foster, S. Q.; Fulweiler, R. W. Estuarine Sediments Exhibit Dynamic and Variable Biogeochemical Responses to Hypoxia. *J. Geophys. Res.: Biogeosci.* **2019**, *124*, 737−758.

(21) Beutel, M.; Leonard, T.; Dent, S.; Moore, B. Effects of aerobic and anaerobic conditions on P, N, Fe, Mn, and Hg accumulation in

waters overlaying profundal sediments of an oligo-mesotrophic lake. *Water Res.* **2008**, *42* (8−9), 1953−1962.
(22) Mortimer, C. Chemical Exchanges Between Sediments and Water in the Great Lakes- Speculations on Probably Regulatory Mechanisms. *Limnol. Oceanogr.* **1971**, *16* (2), 387.
(23) Böstrom, B.; Andersen, J. M.; Fleischer, S.; Jansson, M. Exchange of phosphorus across the sediment-water interface. *Hydrobiologia* **1988**, *170*, 229−244.
(24) Caraco, N. Phosphorus. *Reference Module in Earth Systems and Environmental Sciences: Encyclopedia of Inland Waters* **2009**, 73−78.
(25) Vahtera, E.; Conley, D.; Gustafsson, B.; Kuosa, H.; Pitkänen, H.; Savchuk, O.; Tamminen, T.; Viitasalo, M.; Voss, M.; Wasmund, N.; Wulff, F. Internal Exosystem Feedbacks Enhance Nitrogen-fixing Cyanobacteria Blooms and Complicate Management in the Baltic Sea. *Ambio* **2007**, *36* (2/3), 186−194.
(26) Anderson, H. Internal Phosphorus Loading in Lake Erie's Central Basin. M.S. Thesis, University of Michigan, Ann Arbor, MI, 2020 (https://deepblue.lib.umich.edu/handle/2027.42/155016).
(27) Nowlin, W.; Evarts, J.; Vanni, M. Release rates and potential fates of nitrogen and phosphorus from sediments in a eutrophic reservoir. *Freshwater Biol.* **2005**, *50*, 301−322.
(28) Penn, M.; Auer, M.; Doerr, S.; Driscoll, C.; Brooks, C.; Effler, S. Seasonality in phosphorus release rates from the sediments of a hypereutrophic lake under a matrix of pH and redox conditions. *Can. J. Fish. Aquat. Sci.* **2000**, *57*, 1033−1041.
(29) Wu, Y.; Wen, Y.; Zhou, J.; Wu, Y. Phosphorus Release from Lake Sediments: Effects of pH, Temperature and Dissolved Oxygen. *KSCE Journal of Civil Engineering* **2014**, *18* (1), 323−329.
(30) Rowe, M.; Anderson, E.; Beletsky, D.; Stow, C.; Moegling, S.; Chaffin, J.; May, J.; Collingsworth, P.; Jabbari, A.; Ackerman, J. Coastal Upwelling Influences Hypoxia Spatial Patterns and Nearshore Dynamics in Lake Erie. *J. Geophys. Res.: Oceans* **2019**, *124* (8), 6154.
(31) Burns, N. Temperature, oxygen, and nutrient distribution patterns in Lake Erie, 1970. *J. Fish. Res. Board Can.* **1976**, *33*, 485−511.
(32) Zhou, Y.; Obenour, D.; Scavia, D.; Johengen, T.; Michalak, A. Spatial and Temporal Trends in Lake Erie Hypoxia, 1987−2007. *Environ. Sci. Technol.* **2013**, *47*, 899−905.
(33) Debroux, J.-F.; Beutel, M.; Thompson, C.; Mulligan, S. Design and testing of a novel hypolimnetic oxygenation system to improve water quality in Lake Bard, California. *Lake Reservoir Manage.* **2012**, *28*, 245−254.
(34) Davis, W. S.; Fay, L. A.; Herdendorf, C. E. Lake Erie Intensive Study: Sediment Oxygen Demand. *Ohio State University Report to United States Environmental Protection Agency*; Great Lakes National Program Office: Columbus, OH, 1981.
(35) Burns, N.; Ross, C. Oxygen-nutrient relationships within the central basin of Lake Erie. In *Project Hypo: An Intensive Study of the Lake Erie Central Basin Hypolimnion and Related Surface Water Phenomena*; 1972.
(36) Grand, M.; Clinton-Bailey, G.; Beaton, A.; Schaap, A.; Johengen, T.; Tamburri, M.; Connelly, D.; Mowlem, M.; Achterberg, E. A lab-on-chip phosphate analyzer for long-term *In situ* monitoring at fixed observatories: Optimization and performance evaluation in estuarine and oligotrophic coastal waters. *Front. Mar. Sci.* **2017**, *4* (255), 1−16.
(37) Zorn, M.; Waples, J.; Valenta, T.; Kennedy, J.; Klump, J. V. *In situ* high-resolution time series of dissolved phosphate in Green Bay, Lake Michigan. *J. Great Lakes Res.* **2018**, *44*, 875−882.
(38) WETLabs. Case Studies of WET Labs' Cycle-PO4: Simple and Reliable Nutrient Monitoring. Cycle-PO4 Enabling Novel Science; HydroCycle Phosphate Sensor Datasheet. www.seabird.com (accessed 2020-07-28).
(39) National Oceanic and Atmospheric Administration, Great Lakes Environmental Research Laboratory; Cooperative Institute for Great Lakes Research, University of Michigan. Water physical, chemical, and biological vertical observational data at multiple levels from fixed mooring CHRP2 and CTD casts taken from NOAA research vessel R5501 in the central basin of Lake Erie. Great Lakes region from 2017-06-09 to 2019-10-10 collected by National Oceanic and Atmospheric Administration (NCEI Accession 0210815). Temperature, Depth , 2019. NOAA National Centers for Environmental Information, 2020 (https://accession.nodc.noaa.gov/0210815) (accessed 2020-07-01).
(40) National Oceanic and Atmospheric Administration, Great Lakes Environmental Research Laboratory; Cooperative Institute for Great Lakes Research, University of Michigan. Water current profile, physical, and chemical vertical observational data at multiple levels from fixed mooring CHRP4 and CTD casts taken from NOAA research vessel R5501 in the central basin of Lake Erie, Great Lakes region from 2017-05-23 to 2019-10-10 collected by National Oceanic and Atmospheric Administration, Great Lakes Environmental Research Laboratory and the Cooperative Institute for Great Lakes Research, University of Michigan (NCEI Accession 0210823). Temperature, Depth, 2019. NOAA National Centers for Environmental Information, 2020 (https://accession.nodc.noaa.gov/0210823) (accessed 2020-07-01).
(41) Zhang, H.; Boegman, L.; Scavia, D.; Culver, D. A. Spatial distributions of external and internal phosphorus loads in Lake Erie and their impacts on phytoplankton and water quality. *J. Great Lakes Res.* **2016**, *42*, 1212−1227.
(42) Mason, L.; Riseng, C.; Gronewold, A.; Rutherford, E.; Wang, J.; Clites, A.; Smith, S.; McIntyre, P. Fine-scale spatial variation in ice cover and surface temperature trends across the surface of the Laurentian Great Lakes. *Clim. Change* **2016**, *138*, 71−83.

https://dx.doi.org/10.1021/acsestwater.0c00138
ACS EST Water 2021, 1, 774−781